Journal of NUCLEAR SCIENCE and TECHNOLOGY, Vol. 41, No. 4, p. 448–456 (April 2004)

ORIGINAL PAPER

Neutron and Gamma Ray Source Evaluation of LWR High Burn-up UO_2 and MOX Spent Fuels

Akihiro SASAHARA[1,*], Tetsuo MATSUMURA[1], Giorgos NICOLAOU[2] and Dimitri PAPAIOANNOU[3]

[1]*Central Research Institute of Electric Power Industry, 11-1, Iwado Kita 2-chome, Komae-shi 201-8511 Tokyo*
[2]*National Centre for Scientific Research 'Demokritos', Aghia Paraskevi, 153 10 Athens, Greece*
[3]*European Commission, Joint Research Centre, Institute for Transuranium Elements, P.O. Box 2340, D-76125 Karlsruhe, Germany*

(Received July 7, 2003 and accepted in revised form December 11, 2003)

The axial neutron emission and gamma ray source distribution were measured for LWR high burn-up UO_2 and MOX spent fuel rods. The gamma rays of ^{134}Cs, ^{137}Cs and ^{106}Ru were measured on the fuel rods, and consequently compared with the results of the ORIGEN2/82 calculation, in which both the original library and ORLIBJ32 based on the JENDL-3.2 library were used. The effect of pellet radial gamma distribution on self-shielding factor was considered, and cesium radial migration was also discussed using the ratio of gamma ray intensity of ^{134}Cs to ^{137}Cs. The axial gamma ray measurement and calculation of ^{134}Cs and ^{106}Ru agreed within about 20% and ^{137}Cs agreed within 13% after correction with pellet self-shielding factors. Two types of boundary curves associated with cesium migration were obtained by simple analysis using $^{134}Cs/^{137}Cs$ gamma intensity ratio. The axial neutron emission calculated by ORIGEN2/82 with ORLIBJ32 was generally smaller than the measured ones. The main neutron source in spent fuel is the spontaneous fission of ^{244}Cm. Small buildup of ^{244}Cm caused the underestimation of neutron emission. The main flow up to ^{244}Cm is ^{241}Pu, ^{242}Pu, ^{243}Pu, ^{243}Am and ^{244m}Am. The (n, γ) cross sections of ^{243}Am on the main flow and ^{244}Cm have strong sensitivity on buildup of ^{244}Cm. The re-evaluation of the (n, γ) cross sections of these nuclides will improve the prediction for ^{244}Cm buildup.

KEYWORDS: ***high burn-up uranium dioxide fuel, MOX fuel, ORIGEN2/82, gamma ray source measurement, neutron source measurement, gamma ray self-shielding factor, JENDL-3.2, ORLIBJ32, cesium radial migration***

I. Introduction

The evaluation of neutron emission and gamma ray source distribution in spent fuel is important for the shielding design and criticality safety analysis of spent fuel storage facilities such as dry casks and storage pools. In particular, high burn-up UO_2 and MOX (Pu-thermal) spent fuels have a higher neutron emission than those of conventional burn-up UO_2 fuel as shown **Table 1**. However there are few data on gamma and neutron source distributions for high burn-up UO_2 and MOX spent fuels. In this study, to accumulate appropriate source term data that can be utilized for source evaluation, neutron emission and gamma ray source measurements were carried out on LWR high burn-up UO_2 and MOX spent fuel rods as follows : (1) Axial neutron emission distribution of PWR-UO_2, BWR-UO_2 and PWR-MOX fuel rods, (2) Axial gamma ray source distribution of PWR-UO_2 and PWR-MOX fuel rods, (3) Radial gamma ray source distribution of fuel pellets of PWR-UO_2 and PWR-MOX fuel rods.[1–4)]

Chemical isotopic analyses were also carried out to determine local burn-up and nuclide composition of the fuel rods.[1–3)]

In this study, computational analyses were carried out using the ORIGEN2/82 code.[5)] The libraries used in this study included the original library in the code and the ORLIBJ32[6,7)] library based on JENDL-3.2.[8)] The difference in calculation results caused by the use of different libraries was discussed for the neutron emission and gamma ray source distribution. The effect of radial gamma source profile on self-shielding factor was estimated prior to gamma ray source analysis. The correlation of $^{134}Cs/^{137}Cs$ gamma intensity ratio to cesium radial migration was also discussed. The results indicate that there are the burn-up and the migrated fraction boundaries, which reflect to the minimum burn-up and minimum migrated amount of cesium at the start of cesium migration, respectively.

Table 1 Examples of neuron emission and gamma ray intensity in high burn-up UO_2 and MOX spent fuel calculated using ORIGEN2 code

Source	Conventional UO_2	High burn-up UO_2	MOX
Neutron emission	1.0	1.4	15.1
Gamma ray intensity	1.0	1.1	0.9

*Values are relative to data of conventional UO_2 fuel (initial ^{235}U:4.1 wt%, discharge burn-up:43 MWd/kgHM).

II. Measurement

The analysis of chemical isotopic composition, and measurement of axial neutron emission, and axial and radial gamma ray sources distribution were performed at the Institute for Transuranium Elements (ITU) in Karlsruhe, Germany.

*Corresponding author, Tel.+81-3-3480-2111, Fax.+81-3-3480-2493, E-mail: sasa@criepi.denken.or.jp

Table 2 Sample burn-ups determined by chemical isotopic analyses

Sample	PWR-UO_2[a]	BWR-UO_2[b]		PWR-MOX[c]
	(MWd/kgHM)	(MWd/kgHM)	Void (%)	(MWd/kgHM)
A	64.7	65.6	41.1	46.0
B	52.8	56.4	1.2	46.6
C	60.0	58.8	14.3	
D	63.5	63.8	58.0	

[a]Initial ^{235}U is 3.8%. [b]Initial ^{235}U is 3.5%. [c]Initial Pu is 5.07%.

1. Specification of Fuel and Chemical Isotopic Analysis

The high burn-up UO_2 and MOX spent fuels used in this study were irradiated in commercial PWR and BWR: a high burn-up PWR-UO_2 fuel pin (3.8%^{235}U, 60.2 MWd/kgHM declared average burn-up); a high burn-up BWR-UO_2 fuel pin (3.5%^{235}U, 56 MWd/kgHM declared average burn-up): and two segments (MOX1 and MOX2) from two PWR-MOX fuel pins (5.07% Pu, 44.5 MWd/kgHM and 45.7 MWd/kgHM declared burn-up). The plutonium vector in the MOX fuel used in the fabrication was $^{238}Pu/^{239}Pu/^{240}Pu/^{241}Pu/^{242}Pu/^{241}Am$=1.40/59.05/24.38/6.08/4.86/4.23. The local burn-up achieved at irradiation was calculated on the basis of both the total heavy metal and ^{148}Nd obtained by chemical isotopic analyses. Chemical isotopic analyses were performed on four samples of PWR-UO_2 and BWR-UO_2 fuel respectively, and two samples of PWR-MOX segment fuels. **Table 2** shows the burn-ups determined for each sample by chemical isotopic analyses.

2. Axial Neutron Emission Measurement[9]

The axial distribution of neutron emission was determined using a neutron collar incorporating ^{10}B proportional neutron detectors embedded in a polyethylene moderator. Neutrons emitted from spontaneous fission and (α, n) reactions in the fuel were measured. The efficiency of the collar was calibrated using a ^{252}Cf neutron source. The fuel rod was translated horizontally along the bench on which the collar was mounted and was scanned while passing through the device. The accuracy of the neutron measurement is about 6%.

3. Axial and Radial Gamma Ray Source Measurements

The axial gamma scanning system is based on a Ge detector situated outside a hot cell. The detector is collimated by a vertical slit. The collimator is mounted in the front wall of the hot cell orthogonal to the fuel rod axis, and the slit width was 0.6 mm. The horizontal translation of the fuel rod allows the axial gamma ray source distribution. In this study, gamma energies of 795.8 keV for ^{134}Cs, 661.7 keV for ^{137}Cs and 621.8 keV for ^{106}Ru were measured along the axis of fuel rods.

Pellet radial gamma ray scanning was carried out using a collimated Ge detector to obtain information on the source distribution and migration of ^{134}Cs and ^{137}Cs during irradiation. In the radial scanning, the detection energies of gamma ray were at 604.7 keV for ^{134}Cs and 661.7 keV for ^{137}Cs, respectively. The sample was fixed in a sample holder and the collimator, which is composed of four lead bricks, was adjusted to an area of $1 \times 1\,mm^2$. **Figure 1** shows typical

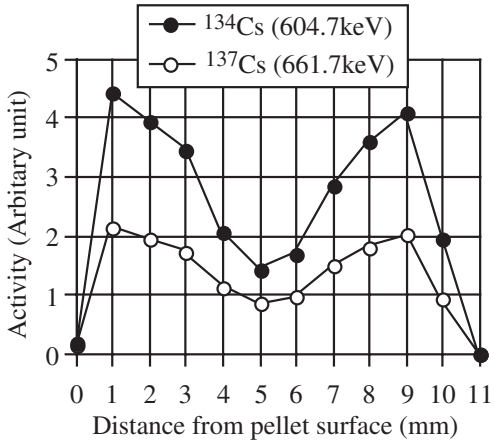

Fig. 1 Cesium radial distribution in PWR-UO_2 pellet obtained by gamma ray measurement

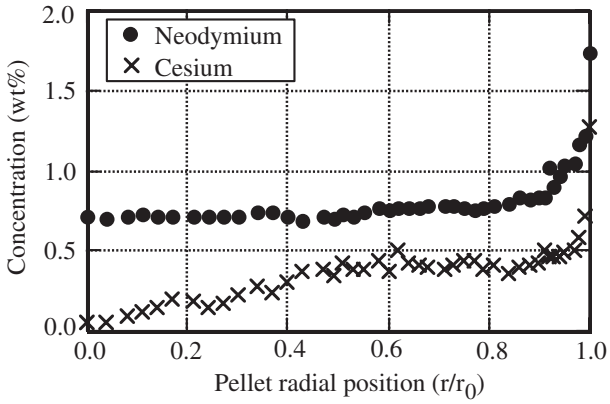

Fig. 2 Cesium and neodymium radial distributions obtained by EPMA on PWR-UO_2 pellet

^{134}Cs and ^{137}Cs radial profiles having a higher activity on the pellet periphery. Cesium migration from the pellet center to colder periphery regions[10] and a steep burn-up increase by a resonance reaction between neutrons and ^{238}U nuclides at pellet surface result in a higher cesium concentration in the pellet periphery region. **Figure 2** shows the neodymium and cesium radial distributions obtained by electron probe microanalysis (EPMA) of the same pellet. Neodymium across the fuel radius provides relative burn-up including the effect of resonance reactions on the pellet surface. To

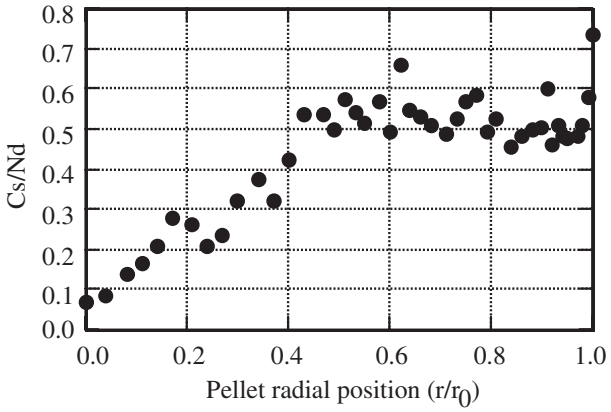

Fig. 3 Ratio of cesium to neodymium radial distributions obtained by EPMA on PWR-UO_2 pellet

correct the effect of local burn-up distribution on cesium distribution, the ratio of cesium to neodymium was estimated as shown in **Fig. 3**. There is still a high cesium concentration in the pellet periphery. This clearly indicates that the high cesium concentration in the pellet periphery in Figs. 1 and 3 is due to cesium migration during irradiation. Thus, prior to the axial gamma evaluation, the effect of cesium radial profile on self-shielding must be discussed.

III. Calculations

1. ORIGEN Calculation and Libraries

Computational analyses were executed using the ORIGEN2/82 code to determine the nuclide compositions of ^{134}Cs, ^{137}Cs and ^{106}Ru, as well as the neutron emission at the fuel axial position at which local burn-up had been determined by chemical analysis. The measurement results were compared with the calculations in which original ORIGEN libraries and ORLIBJ32 libraries were used. The burn-up profile of BWR-UO_2 fuel rod is affected by axial void distribution during irradiation, which in turn affects fuel nuclide composition. To allow for void distribution, three libraries with void fractions of 0%, 40% and 70% prepared in ORLIBJ32 were used for the analyses of each sample and the calculation results obtained from each library were interpolated at a corresponding axial void fraction (Table 2). **Table 3** shows the summary of the libraries used in this study.

Table 3 Libraries used in the calculation

Reactor	Original libraries	ORLIBJ32 libraries
PWR-UO_2	PUD50	PWR34J32
BWR-UO_2	BWRU	BS200J32, BS240J32, BS270J32
PWR-MOX	PWRPUPU	PWRM205

2. Effect of Cesium Radial Profile on Gamma Intensity

Cesium migration occurs from the hotter center region to the colder peripheral pellet region (Fig. 1) caused by cesium high vapor pressure. Thus, the effect of cesium profile in a pellet on self-shielding factor and the consequently measured gamma intensity were evaluated using asymptotic profiles, namely, (1) flat profile, (2) well profile and (3) sloping profile. **Figure 4** shows the source term profiles using the evaluation of the self-shielding factor. The mass attenuation coefficients[11] of uranium and oxygen for UO_2 and MOX pellets, and molybdenum, instead of zirconium, for cladding were used in the calculation. The attenuation coefficients of UO_2 and MOX pellets, considering fuel density change due to irradiation, and cladding region are shown in **Table 4**. The gamma intensity of the UO_2 pellet was calculated for each asymptotic radial profile of ^{134}Cs, ^{137}Cs and ^{106}Ru, and the differences between the gamma intensities based on the sloping profile are shown in **Table 5**. In the calcula-

Table 4 Attenuation coefficients of UO_2 and MOX pellet, and cladding

Fission product	Energy (keV)	UO_2 (cm^{-1})	MOX (cm^{-1})	Cladding (cm^{-1})
^{106}Ru	621.8	1.315	1.316	0.493
^{134}Cs	604.7	0.976	0.977	0.499
	795.8	0.964	0.965	0.428
^{137}Cs	661.7	1.235	1.235	0.478

Table 5 Effect of pellet radial source profile on gamma intensity

Gamma source	((1)[a]–(3)[a]) ×100/(3), %	((2)[a]–(3)) ×100/(3), %
^{106}Ru	−0.90	0.57
^{134}Cs	−0.94	0.58
^{137}Cs	−0.81	0.56

[a](1), (2) and (3) mean flat profile, well profile and sloping profile, respectively.

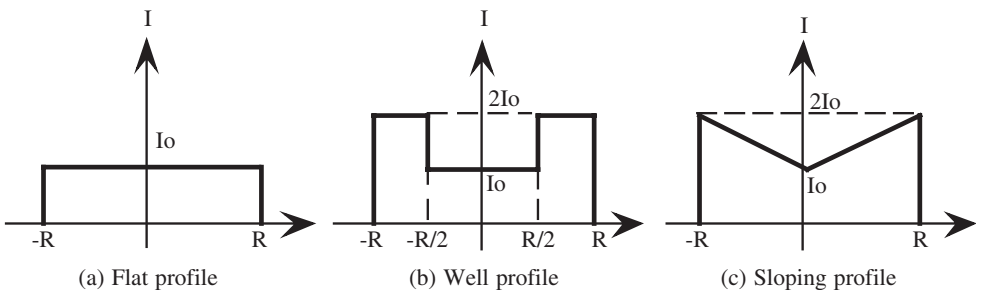

(a) Flat profile (b) Well profile (c) Sloping profile

Fig. 4 Asymptotic radial profiles of cesium and ruthenium in pellet used for evaluation of self-shielding factor

Table 6 Self-shielding factors of PWR-UO_2 and PWR-MOX pellet determined by calculation

Nuclide	Self-shielding factor of PWR-UO_2 and PWR-MOX fuel
^{134}Cs (604.7 keV)	0.596
^{134}Cs (795.8 keV)	0.678
^{137}Cs (661.7 keV)	0.619
^{106}Ru (621.8 keV)	0.597

tions, a simple exponential formula was applied to the attenuation of gamma rays passing through the pellet and cladding region:

$$I = \iint_R S(x, y) \exp[-\mu l(x, y)] dx dy,$$

where I: Gamma intensity from pellet
$S(x, y)$: Pellet radial profile of gamma source
μ: Attenuation coefficient
$l(x, y)$: Path length in pellet
R: Pellet region.

Although a higher cesium concentration in pellet periphery region shows a higher gamma intensity, the difference between the gamma intensity of the sloping profile and those of other profiles is less than $\pm 1\%$. Considering that cesium in fuel can migrate to the colder periphery pellet region during irradiation and ruthenium cannot, the sloping profile was regarded as a cesium distribution profile and the flat profile as a ruthenium distribution profile of the pellet, for calculation purposes.

The self-shielding factor for each gamma energy and profile were calculated. The results are shown in **Table 6**. The attenuation of gamma intensity in the pellet is from 32% to 40% at the range of these gamma energies.

IV. Evaluation of Calculated Results and Discussion

1. Axial Gamma Ray Distribution

Figure 5 shows the distributions of ^{134}Cs, ^{137}Cs and ^{106}Ru obtained by measurement, as well as the calculated values at four axial positions (A–D). There is a small significant difference between ORIGEN original and ORLIBJ32 libraries in the calculation.

Table 7 shows the experimental and calculated axial gamma ray sources of PWR-UO_2. The C/E (ratio of calculation to experimental result) is also shown in the table. Samples A and D correspond to the axial central region in which the burn-up distribution is almost flat. Samples B and C correspond to the axial upper and lower regions in which the burn-up markedly changed. The burn-ups used in the calculation were obtained by chemical isotopic analyses of pellet-wise samples and they were average values for the samples. Therefore, it is expected that the burn-up using calculation is somewhat different from the actual local burn-up at each gamma measurement position, particularly in the axial upper and lower regions. Although the results obtained directly by

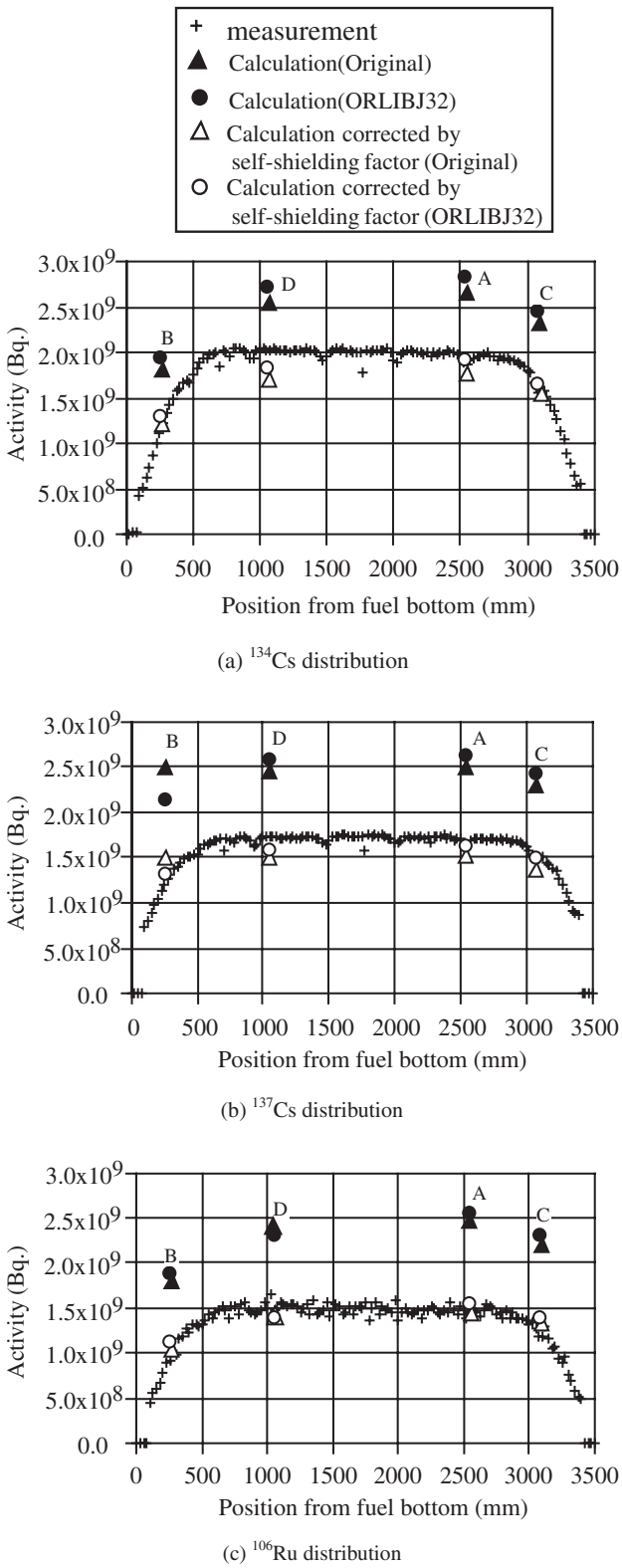

Fig. 5 Measured and calculated gamma ray source distributions along fuel rod

ORIGEN calculation were about twice larger than the experimental results, the calculations corrected with the pellet self-shielding factor were well improved. The calculation results at the central region agreed within about 15% of the measurement results, while those at the upper and lower re-

Table 7 Measured and calculated gamma ray source along PWR-UO_2 fuel rod

Sample (MWd/kgHM)		Measurement (Bq)	Calculation (Bq)		Calculation corrected by self-shielding factor (Bq)		C/E	
			Original	ORLIBJ32	Original	ORLIBJ32	Original	ORLIBJ32
A(64.7)	^{106}Ru	1.395×10^{9}	2.539×10^{9}	2.577×10^{9}	1.516×10^{9}	1.539×10^{9}	1.09	1.10
	^{134}Cs	1.878×10^{9}	2.701×10^{9}	2.849×10^{9}	1.831×10^{9}	1.931×10^{9}	0.97	1.03
	^{137}Cs	1.661×10^{9}	2.554×10^{9}	2.640×10^{9}	1.580×10^{9}	1.633×10^{9}	0.95	0.98
B(52.8)	^{106}Ru	9.237×10^{8}	1.871×10^{9}	1.903×10^{9}	1.117×10^{9}	1.136×10^{9}	1.21	1.23
	^{134}Cs	1.082×10^{9}	1.896×10^{9}	1.952×10^{9}	1.285×10^{9}	1.323×10^{9}	1.19	1.22
	^{137}Cs	1.175×10^{9}	2.085×10^{9}	2.153×10^{9}	1.290×10^{9}	1.332×10^{9}	1.10	1.13
C(60.0)	^{106}Ru	1.196×10^{9}	2.283×10^{9}	2.320×10^{9}	1.363×10^{9}	1.385×10^{9}	1.14	1.16
	^{134}Cs	1.570×10^{9}	2.374×10^{9}	2.479×10^{9}	1.609×10^{9}	1.680×10^{9}	1.02	1.07
	^{137}Cs	1.504×10^{9}	2.361×10^{9}	2.440×10^{9}	1.461×10^{9}	1.510×10^{9}	0.97	1.00
D(63.5)	^{106}Ru	1.505×10^{9}	2.437×10^{9}	2.476×10^{9}	1.455×10^{9}	1.478×10^{9}	0.97	0.98
	^{134}Cs	2.042×10^{9}	2.603×10^{9}	2.738×10^{9}	1.764×10^{9}	1.856×10^{9}	0.86	0.91
	^{137}Cs	1.728×10^{9}	2.505×10^{9}	2.588×10^{9}	1.550×10^{9}	1.601×10^{9}	0.90	0.93

Table 8 Measured and calculated gamma ray source of PWR-MOX fuel rod

Sample (MWd/kgHM)		Measurement (Bq)	Calculation (Bq)		Calculation corrected by self-shielding factor (Bq)		C/E	
			Original	ORLIBJ32	Original	ORLIBJ32	Original	ORLIBJ32
A(46.0)	^{106}Ru	8.074×10^{8}	1.420×10^{9}	1.450×10^{9}	8.469×10^{8}	8.648×10^{8}	1.05	1.07
	^{134}Cs	8.232×10^{8}	9.961×10^{8}	1.052×10^{9}	6.744×10^{8}	7.123×10^{8}	0.82	0.87
	^{137}Cs	1.222×10^{9}	1.796×10^{9}	1.867×10^{9}	1.110×10^{9}	1.154×10^{9}	0.91	0.94
B(46.6)	^{106}Ru	8.240×10^{8}	1.432×10^{9}	1.462×10^{9}	8.541×10^{8}	8.723×10^{8}	1.04	1.06
	^{134}Cs	8.630×10^{8}	1.018×10^{9}	1.074×10^{9}	6.891×10^{8}	7.272×10^{8}	0.80	0.84
	^{137}Cs	1.253×10^{9}	1.816×10^{9}	1.887×10^{9}	1.123×10^{9}	1.166×10^{9}	0.90	0.93

gions agreed within about 20%. **Table 8** also shows the experimental and calculated axial gamma ray sources of PWR-MOX segments. The gamma ray source distribution in the PWR-MOX segment is almost flat. For PWR-UO_2, PWR-MOX and BWR-UO_2, the measurement and calculation results of ^{137}Cs agreed within 13%. For ^{134}Cs and ^{106}Ru, the agreement was about 20%. The gamma ray source analysis along the fuel rod shows that self-shielding effects markedly on the evaluation of gamma intensity.

2. Radial ^{134}Cs/^{137}Cs Gamma Intensity Ratio

The radial gamma ray source distribution shown in Fig. 1 indicates that ^{134}Cs and ^{137}Cs migrate to a colder pellet periphery during irradiation. The gamma intensity ratio of ^{134}Cs to ^{137}Cs is used as a burn-up indicator of fuel because it has good correlation with burn-up increase.[12] If cesium migration occurs in the pellet, the ratio of ^{134}Cs to ^{137}Cs is smaller. In **Fig. 6**, there is a decrease in the measurement ^{134}Cs/^{137}Cs gamma intensity ratio at the pellet center region associated with cesium migration. Cesium-134 is generated indirectly through the (n,γ) reaction with ^{133}Cs produced by fission. On the other hand, ^{137}Cs is generated directly by fission. Thus if cesium migration occurs, ^{137}Cs is generated immediately by fission and accumulates again, but the accumulation of ^{134}Cs resulting from the capture reaction of ^{133}Cs, which is directly generated by fission, is delayed, consequently resulting in a smaller ^{134}Cs/^{137}Cs gamma intensity ratio as shown in Fig. 6. It has not been investigated what information can be derived from the change in ^{134}Cs/^{137}Cs gamma intensity ratio regarding fuel irradiation history, whereas the change in the ^{134}Cs/^{137}Cs gamma intensity

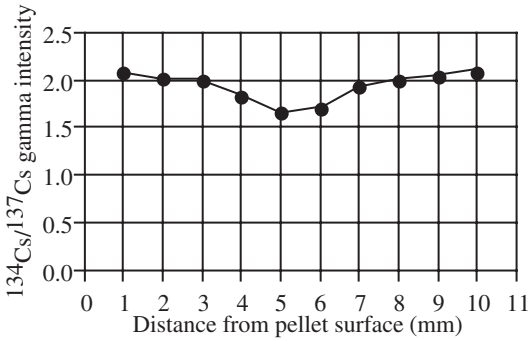

Fig. 6 Effect of radial cesium migration on ^{134}Cs/^{137}Cs gamma intensity ratio obtained by measurement for PWR-UO_2 pellet

ratio indicates cesium migration during irradiation and affects the estimation of fuel burn-up. Hence the correlation between burn-up, migrated fraction at the start of cesium migration during irradiation and $^{134}Cs/^{137}Cs$ gamma intensity ratio was examined by simple calculation.

In the calculation, ^{235}U, ^{239}Pu and ^{241}Pu were considered as fissile nuclides that generate ^{133}Cs, ^{134}Cs and ^{137}Cs through

$$\frac{dN_{Cs133}}{dt} = \gamma_{Cs133} \sum_{f,Cs133} \phi - \sigma_{\gamma,Cs133} N_{Cs133} \phi,$$

$$\frac{dN_{Cs134}}{dt} = \sigma_{\gamma,Cs133} N_{Cs133} \phi - \lambda_{Cs134} N_{Cs134} - \sigma_{\gamma,Cs134} N_{Cs134} \phi,$$

$$\frac{dN_{Cs137}}{dt} = \gamma_{Cs137} \sum_{f,Cs137} \phi - \lambda_{Cs137} N_{Cs137} - \sigma_{\gamma,Cs137} N_{Cs137} \phi,$$

where $\gamma_{Cs133} \sum_{f,Cs133} = \gamma_{Cs133,U235} \sum_{f,U235} + \gamma_{Cs133,Pu239} \sum_{f,Pu239} + \gamma_{Cs133,Pu241} \sum_{f,Pu241}$

$\gamma_{Cs137} \sum_{f,Cs137} = \gamma_{Cs137,U235} \sum_{f,U235} + \gamma_{Cs137,Pu239} \sum_{f,Pu239} + \gamma_{Cs137,Pu241} \sum_{f,Pu241}$

$\gamma_{i,j}$: yield of nuclide i from fission reaction of nuclide j

$\sum_{f,j}$: macroscopic fission cross section of nuclide j

$\sigma_{\gamma,j}$: microscopic capture cross section of nuclide j

λ_j: decay constant of nuclide j

N_j: number density of nuclide j

ϕ: Neutron flux.

The cross sections of ORLIBJ32 were used as the microscopic cross sections of cesium and fissile nuclides, and the number density of fissile nuclides and neutron flux were obtained by ORIGEN calculation with ORLIBJ32. The fission yield data adopted were the values in Ref. 13). **Figure 7** shows the burn-up dependency of $^{134}Cs/^{137}Cs$ gamma intensity ratio for PWR-UO_2 calculated using ORIGEN with ORLIBJ32. The result obtained by the simple calculation agrees well with the ORIGEN calculation result. The effects of burn-up when cesium migration starts and the migrated fraction of cesium on $^{134}Cs/^{137}Cs$ gamma intensity ratio were examined by the simple calculation. Consequently the relationships between the burn-up, the migrated fractions of cesium at the start of migration and $^{134}Cs/^{137}Cs$ gamma intensity ratio were derived for the PWR-UO_2 and PWR-MOX fuels.

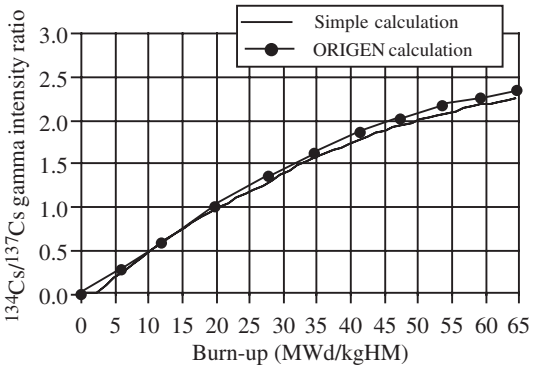

Fig. 7 Calculated $^{134}Cs/^{137}Cs$ gamma intensity ratio, as a function of burn-up, obtained by simple calculation and ORIGEN calculation

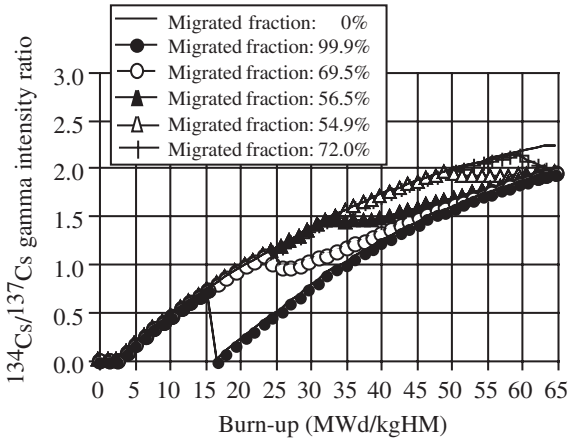

Fig. 8 Dependency of calculated $^{134}Cs/^{137}Cs$ gamma intensity ratio on burn-up and migrated fraction

As example of the calculation results, **Fig. 8** shows the behavior of $^{134}Cs/^{137}Cs$ gamma intensity ratio in the cases that the burn-ups of cesium migration start are 16.8, 24.6, 33.7, 50.5 and 60.9 MWd/kgHM, and the range of migrated fraction is 54.9 to 99.9% of the amount of cesium accumulated during irradiation. For 99.9% migration at 16.8 MWd/kgHM, 99.9% of cesium that accumulated during irradiation migrated and then the $^{134}Cs/^{137}Cs$ gamma intensity ratios decreased to almost zero because ^{137}Cs accumulated immediately after migration but the accumulation of ^{134}Cs, which was generated by the capture reaction of ^{133}Cs, was delayed. The absolute amount of residual cesium at high burn-ups is larger than that of cesium at low burn-ups even if the same fraction of accumulated cesium migrates at some burn-up. Hence, the effect of cesium that is generated again after migration on $^{134}Cs/^{137}Cs$ gamma intensity ratio becomes smaller at higher burn-ups and consequently the change in $^{134}Cs/^{137}Cs$ gamma intensity ratio decreases.

The $^{134}Cs/^{137}Cs$ gamma intensity ratios shown in Fig. 8 at 65 MWd/kgHM obviously show a range of burn-up and migrated fraction. For example, a $^{134}Cs/^{137}Cs$ gamma intensity ratio of 1.95 at a burn-up of 65 MWd/kgHM corresponds to not only the migration that occurred at a burn-up beyond 16.8 MWd/kgHM but also the migrated fraction of more than 54.9% of the accumulated cesium. Cesium migration boundary curves obtained by the simple calculation are shown in **Figs. 9** and **10**. Figure 9 shows the correlation between the lowest normalized burn-up at the start of cesium migration and the decrease in $^{134}Cs/^{137}Cs$ gamma intensity ratio. Figure 10 shows the correlation curve between the minimum fraction of cesium migration and $^{134}Cs/^{137}Cs$ gamma intensity ratio. If the $^{134}Cs/^{137}Cs$ gamma intensity ratio in discharged fuel is 40% smaller than that expected, then the cesium migration corresponds to a 40% decrease in $^{134}Cs/^{137}Cs$ gamma intensity ratio that causes in normalized burn-up of more than 0.55, simultaneously, more than 85% of the accumulated cesium migrates during irradiation.

This correlation between the lowest normalized burn-up at

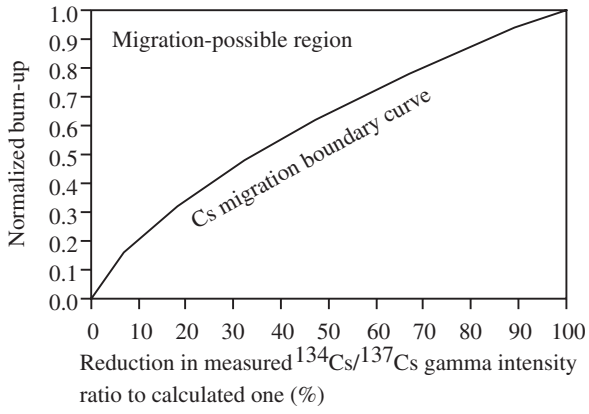

Fig. 9 The correlation between lowest normalized burn-up at the start of cesium migration and $^{134}Cs/^{137}Cs$ gamma intensity ratio
Normalized burn-up means the ratio of burn-up at start of cesium migration to discharged burn-up.

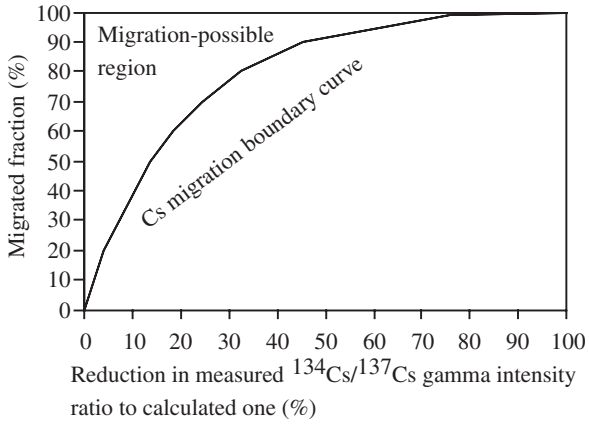

Fig. 10 The correlation between the minimum fraction of cesium migration and $^{134}Cs/^{137}Cs$ gamma intensity ratio

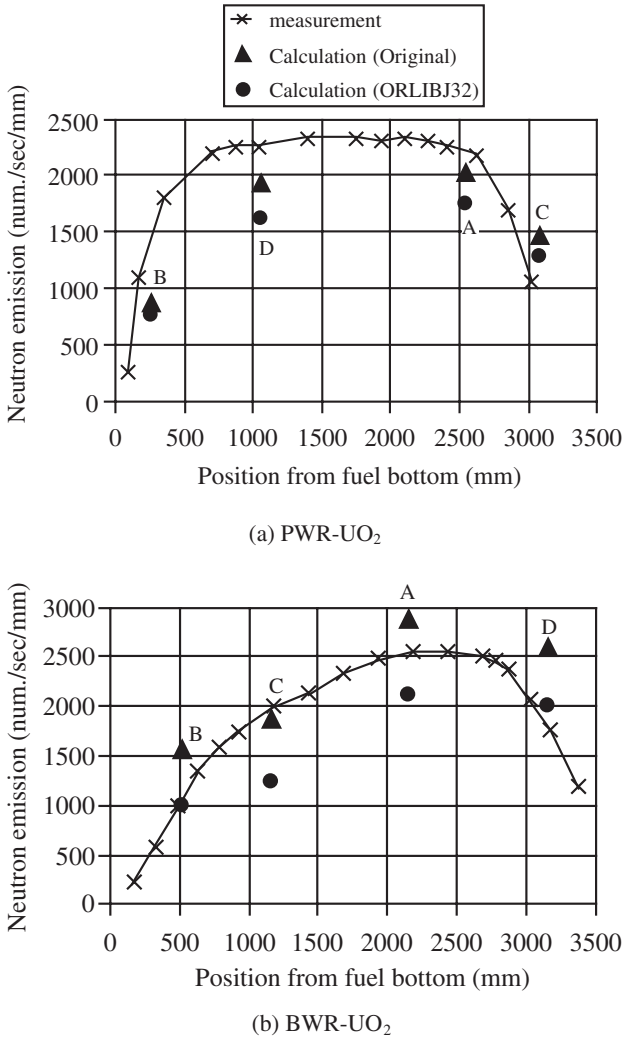

Fig. 11 Measured and calculated neuron emission distributions along fuel rod

the start of cesium migration, the minimum fraction of cesium migration and the decrease in $^{134}Cs/^{137}Cs$ gamma intensity ratio is valid for LWR-UO_2 and MOX fuel, because the fission yields from ^{235}U, ^{239}Pu and ^{241}Pu to ^{133}Cs and ^{137}Cs are almost the same values.[13)]

Hence, the lowest burn-up and minimum migrated fraction at the cesium migration start can be estimated from the change in $^{134}Cs/^{137}Cs$ gamma intensity ratio using the cesium migration boundary curves for LWR fuels.

3. Axial Neutron Distribution

Measured and calculated neutron emissions, as functions of distance along the active length of fuel rod, are shown in **Fig. 11**. There was a discrepancy between the measurement and calculation results depending on whether the library used was the original ORIGEN or ORLIBJ32. In particular, the calculation results using ORLIBJ32 were generally, smaller than the measurement results. The differences between the measurement and calculated axial neutron emissions are shown in **Table 9**. In the calculation, neutrons from spontaneous fission and (α, n) reaction were considered as those emitted from the fuel rod. The main neutron source after a few years of cooling is the spontaneous fission from ^{244}Cm, which produces more than 94% in total neutron emission in this case. The uncertainty in the half-life of spontaneous fission of ^{244}Cm is 1.31×10^7 to 1.35×10^7 yr and that in emission number (ν) is 2.61 to 2.72. The effect of these uncertainties on the number of neutron is less than 5%. Thus, underestimation of neutron emission in the calculation is mainly due to smaller buildup of ^{244}Cm. **Figure 12** shows the transmutation flow from ^{238}Pu to ^{244}Cm, and the transmutation and decay ratios obtained using ORIGEN with the ORLIBJ32 library. The main flow up to ^{244}Cm is ^{241}Pu, ^{242}Pu, ^{243}Pu, ^{243}Am and ^{244m}Am as shown in Fig. 12. The sensitivity analysis by the use of ORIGEN with the ORLIBJ32 library was performed to define important nuclides that affect buildup of ^{244}Cm. There is a small discrepancy between measurement and calculation results of plutonium.[14,15)] The results indicated that the (n, γ) cross sections of ^{243}Am on the main flow and ^{244}Cm have strong sensitivity on buildup of ^{244}Cm. The re-evaluation of the (n, γ) cross sections of both nuclides will improve the prediction for ^{244}Cm buildup.

Table 9 Measured and calculated neutron emission along PWR-UO_2, BWR-UO_2 and PWR-MOX fuel rods

Sample	Measurement	Calculation (n/s/mm)		Difference (%)	
(MWd/kgHM)	(n/s/mm)	Original	ORLIBJ32	Original	ORLIBJ32
(a) PWR-UO_2					
A(64.7)	2,220	2,047	1,763	−7.8	−20.6
B(52.8)	1,406	896	785	−36.3	−44.2
C(60.0)	770	1,491	1,291	96.6	67.7
D(63.5)	2,245	1,945	1,643	−13.4	−26.8
(b) BWR-UO_2					
A(65.6)	2,541	2,909	2,128	14.5	−16.2
B(56.4)	1,054	1,592	1,016	51.0	−3.6
C(58.8)	1,965	1,893	1,266	−3.7	−35.6
D(63.8)	1,861	2,625	2,035	41.0	9.4
(c) PWR-MOX					
A(46.0)	4,582	4,728	3,951	3.2	−13.8
B(46.6)	5,176	4,838	4,032	−6.5	−22.1

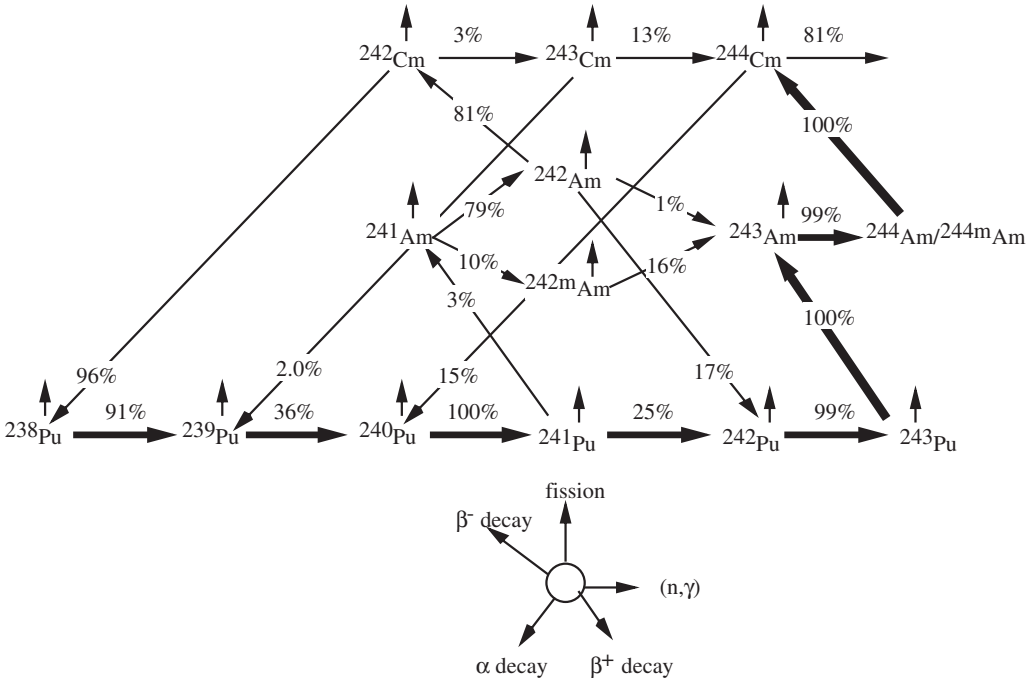

Fig. 12 Predominant path up to ^{244}Cm and transmutation ratio

V. Conclusions

To accumulate appropriate source term data that can be utilized for source evaluation, axial neutron emission and gamma ray source distribution measurements of fuel rods were performed on LWR high burn-up UO_2 and MOX spent fuel rods. Chemical isotopic analyses of the fuel rods at different axial positions were also carried out to determine local burn-up and nuclide composition. In gamma ray measurement, ^{134}Cs, ^{137}Cs and ^{106}Ru as gamma sources were measured for the fuel rods and consequently compared with the results obtained by the ORIGEN2/82 calculation, in which both the original library and ORLIBJ32 based on JENDL-3.2 library were used. Axial neutron emission was also compared with that obtained by ORIGEN2/82 calculation.

(1) Although the gamma intensity obtained directly by ORIGEN calculation were about twice larger than that measurement results, the calculation results for ^{137}Cs, ^{134}Cs and ^{106}Ru, corrected with the pellet self-shielding factor agreed within 13%, 22% and 23%, respectively. The gamma ray source analysis of the fuel rod showed that self-shielding effects markedly on the evaluation of the gamma intensity.

(2) ^{134}Cs and ^{137}Cs migrations in a pellet during irradiation cause a reduction in $^{134}Cs/^{137}Cs$ gamma intensity ratio. The effects of a burn-up when cesium migration starts

and the migrated fraction of cesium on $^{134}Cs/^{137}Cs$ gamma intensity ratio were examined by simple calculation for PWR-UO_2 and PWR-MOX fuels. As a result, cesium migration boundary curves were obtained. These curves indicate the lowest normalized burn-up at the start of cesium migration and the minimum fraction of cesium migration.

(3) The calculation results using ORLIBJ32 were generally smaller than the measurement results. The underestimation of neutron emission is mainly due to smaller buildup of ^{244}Cm in the calculation. The main transmutation flow up to ^{244}Cm was clearly defined using ORIGEN with ORLIBJ32. The sensitivity analysis by the use of ORIGEN with the ORLIBJ32 library showed that the (n, γ) cross sections of ^{243}Am on the main flow and ^{244}Cm have strong sensitivity on buildup of ^{244}Cm. The re-evaluation of the (n, γ) cross section of both nuclides will improve the prediction for ^{244}Cm buildup.

References

1) A. Sasahara, T. Matsumura, G. Nicolaou, *Post Irradiation Examinations and the Validity of Computational Analysis for High Burn-up UO_2 and MOX Spent Fuels*, CRIEPI report, T95012, (1996), [in Japanese].
2) A. Sasahara, T. Matsumura, G. Nicolaou, *et al.*, ''Post irradiation examinations and computational analysis of high burnup UOx and MOX spent fuels for interim dry storage,'' *Proc. Int, Conf. 10th Pacific Basin Nuclear Conf.*, Kobe, Oct. 20–25, 1996, p. 1073 (1996).
3) A. Sasahara, T. Matsumura, G. Nicolaou, *et al.*, ''Post irradiation examinations of MOX spent fuel for interim dry storage,'' *Proc. Int. Conf. Future Nuclear Systems*, Yokohama, Oct. 5–10, 1997, p. 504 (1997).
4) T. Matsumura, A. Sasahara, G. Nicolaou, *et al.*, ''Neutron/gamma ray source measurement and analyses of high burnup UO_2/MOX fuel rods,'' *J. Nucl. Sci. Technol.*, Supplement 1, pp. 580–583 (2000).
5) A. G. Croff, *A User's Manual for the ORIGEN2 Computer Code*, ORNL/TM-7175, Oak Ridge National Laboratory, (1980).
6) K. Suyama, J. Katakura, Y. Ohkawachi, *et al.*, *Libraries Based on JENDL-3.2 Code: ORLIBJ32*, JAERI-Data/Code 99-003, Japan Atomic Energy Research Institute, (1999), [in Japanese].
7) K. Suyama, M. Onoue, H. Matsumoto, *et al.*, *ORIGEN2 Libraries Based on JENDL-3.2 for LWR-MOX Fuels*, JAERI-Data/Code 2000-036, Japan Atomic Energy Research Institute, (2000), [in Japanese].
8) T. Nakagawa, K. Shibata, S. Chiba, *et al.*, ''Japanese evaluated nuclear data library version 3 revision-2: JENDL-3.2,'' *J. Nucl. Sci. Technol.*, **32**, 1259–1271 (1995).
9) G. Nicolaou, L. Koch, ''Characterization of spent nuclear fuel by non-destructive assay,'' *Radioactive Waste Management and Environmental Remediation*, ASME, (1995).
10) T. K. Campbell, R. J. Guenther, E. D. Jenson, *Volatile Fission Product Distributions in LWR Spent Fuel Rods*, PNL-SA-16483, (1989).
11) J. H. Hubbell, *Photon Cross Sections, Attenuation Coefficients, and Energy Absorption Coefficients from 10 keV to 100 keV*, NSRDS-NBS 29, (1969).
12) H. Graber, G. Hofmann, R. Berndt, *Correlations of Burnup with the $^{134}Cs/^{137}Cs$ and $^{154}Eu/^{137}Cs$ Concentration Ratios for Irradiated LWR Fuel*, IAEA-SM-260/84, (1983).
13) K. Tasaka, J. Katakura, H. Ihara, *et al.*, *JNDC Nuclear Data Library of Fission Products—second version—*, JAERI 1320, Japan Atomic Energy Research Institute, (1990).
14) K. Okumura, ''Post irradiation examination analysis of LWR high burn-up UO_2 fuels by the use of JENDL, JEF and ENDF/B,'' *Kaku-Data-News (Japan At. Energy Res. Inst.)*, **74**, 39 (2003), [in Japanese].
15) S. Cathalau, A. Benslimane, ''Qualification of JEF2.2 capture cross-sections for heavy nuclides and fission products in thermal and epithermal spectra,'' *Proc. Int. Conf. Evaluation of Emerging Nuclear Fuel Cycle Systems*, Versailles, France, Sep. 11–14, 1995, p. 1537 (1995).